Effect of substrate type and optimization of the preparation condition for PbSnTe films used as IR photoconductors

M. A. RAFEA[*], R. LABUSCH[a], F. S. TERRA[b], M. MOUNIR[c]

Institute of Advanced Technology & New Materials, Mubarak City for Scientific Research & Technology Applications, P.O. Box 21934 Universities and Research Centers District, New Borg El Arab City, Alexandria, Egypt
[a]*Solid State Physics Dep., National Research Centre, Dokki, Cairo, Egypt*
[b]*Institute of Applied Physics and Technology, TU-Clausthal, Germany*
[c]*Physics Department, Faculty of Science ,Cairo University*

$Pb_{0.85}Sn_{0.15}Te$ was prepared from its constituent pure elements by melting in helium atmosphere under vacuum of 10^{-3} Torr. Thin films were deposited from this ingot materials by electron beam evaporation technique on glass and mono-crystalline substrates of KBr, CaF_2, mica sheets and BaF_2 at substrate temperature 573 K. The films were annealed at 723 K for one hour. The composition of the films are close to the ingot material composition while excess Te was observed the crystallographic orientation [200] was observed to be preferred during the growth process of the film. Hall mobility of the films was observed to be lower than of the mobility of the single crystal. p-type carrier concentration of ~10^{18} cm^{-3} at 300 K. Cooling heating cycles process was applied to the films from 100-300 K. The dark and photoconductivity were measured in the same temperature range. It was found the films change due to cooling-heating process. This was discussed briefly and the difference of the thermal expansion coefficient and thermal conductivity between the films and the substrates was pointed out. A model of films-substrates matching was suggested and relations were deduced. It results that the thermally expansion coefficient of the films and the substrates should be close to each other for epitaxial growth. Different substrates with different thermal expansion coefficient, structure, surface properties and unit cell dimension was used in order to verify our suggested model. It was found that the Hall mobility dark conductivity and photoconductivity increase sharply and approach the values of the PbSnTe single crystal for films deposited on single crystalline substrates. The measurements of Hall mobility shows that the carriers are scattered by acoustic phonons. The band gap photoconductivity of the films was measured at different compositions and temperatures under monochromatic IR radiation and the band gap were determined. The results agree well with the theoretical data.

(Received June 04, 2009; accepted June 15, 2009)

Keywords: PbSnTe, Thin films, Structure, Photoconductivity, Band gap, Substrate type

1. Introduction

PbSnTe is an important material for wide applications in IR spectroscopy, detectors, night vision, Photodiodes, IR photoconductors and detectors. $Pb_{1-x}Sn_xTe$ has cubic structure with lattice dimensions, a(Å), at x=0.0 and x=1.0 of 6.454 and 6.313 Å, respectively. The lattice dimension of the $Pb_{1-x}Sn_xTe$ follows the Végard`s low [1-3].

$$a(x) = (1-x)\times 6.454 + x\times 6.313 \text{ Å}. \quad \text{At x=0.15,}$$
$$a = 6.433 \text{ Å}.$$

Single crystal [4] of PbTe was grown by Bridgman method on the crystallographic orientations (200), (400). Epitaxial films of PbTe [5,6] were prepared on NaCl crystals cleaved at (001) plane and porous Si, the films was examined by electron and optical microscopy showing the absence of pores and cracks. Cooling-heating cycles at temperature range 77-300 K did not lead to the process of peeling or appearance of crakes, although there is a large difference in thermal expansion coefficient between Si and

PbTe. Deposition on thick amorphous Si layer substrate changes the growth properties of the PbTe films. Indium doped $Pb_{0.83}Sn_{0.17}Te$ films [7] have been prepared by the hot wall technique. The Hall mobility at 12 K was in the range $(2-3)\times 10^5$ cm^{2}V^{-1}s^{-1} for n-type, while it was in the range $(6-8)\times 10^5$ cm^{2}V^{-1}s^{-1} for p-type films. A positive temperature coefficient of the band gap was observed. The carriers concentration of the samples was 3×10^{18} cm^{-3}. Bismuth doped $Pb_{0.8}Sn_{0.2}Te$ single crystal was prepared with different doping concentration in the range 0-10^{21} cm^{-3} [8]. The resultant carrier concentration changes from p-type at $p\sim 10^{20}$ to n-type at $n\sim 10^{20}$cm^{-3}. At 77 K, the Hall mobility decreases monotonically with carrier concentration from 6×10^4 to 4×10^2 cm^{2}V^{-1}s^{-1}. At 300 K, the Hall mobility is independent on the carriers concentration, which is equal 10^3 cm^{2}V^{-1}s^{-1} at n or $p\leq 10^{19}$ cm^{-3}. At n or $p > 10^{19}$, the mobility decreases sharply to 10^2 cm^{2}V^{-1}s^{-1} and the ionized impurity scattering is dominant at 77 and 300 K. Hall mobility at carrier concentration range 10^{17}-10^{19} cm^{-3} was characterized by acoustic phonon

scattering at 300 K and either ionized impurity or mixed scattering was obtained at 77 K. P-type $Pb_{0.82}Sn_{0.18}Te$ single crystals [9], the carriers was p-type, their concentration was in the range from 2.14×10^{15}-7×10^{15} cm^{-3} and the mobility was 10^6 cm^{2}V^{-1}s^{-1} below 10 K. PbTe:Bi/$Pb_{0.8}Sn_{0.2}Te$ photo-detectors [10] were prepared on Si(100) substrate by hot wall epitaxy. The detector working temperature was 300 K. The samples contained tensile strain parallel to the interface, which was explained by the large difference in thermal expansion coefficient and a considerable difference in lattice constants of Si and PbTe. Pb/PbTe diode and n-PbTe:Bi/p-PbTe p-n junction were prepared as photodiode detector [11-14] on Si substrate. A buffer layers made from CaF$_2$-BaF$_2$ was found to increase the detector characteristics and performance. In this work, we study the effect of substrate type on the photoconductivity and film characteristics and what is the best substrate which produces high performance photoconductor detectors of PbSnTe.

2. Experimental

$Pb_{0.85}Sn_{0.15}Te$ ingot material was prepared in evacuated silica ampoules under pressure 10^{-6}-10^{-7} Torr. Pure He gas is passed through the silica ampoule in order to reduce the vacuum to 1 mTorr. The purity of the constituent elements Pb, Sn and Te was 6N (Alfa Aesar Johnson Matthey GmbH Germany). A balance of accuracy 0.0001g was used. The closed ampoule was placed in a furnace at 1223±5 K and a calibrated thermocouple (Chromel-Alumel) was fixed at the melting zone of the ampoule beside the thermocouple of the temperature controller of the furnace. The ampoule is then gradually moved downwards in the furnace until the mixture was completely melted for two hours with shaking every 10 min. The temperature was decreased rapidly below the melting point to 1073 K in order to solidify the material from the liquid state and prevents segregation. The ampoule is kept inside the furnace which is turned off and the room temperature was reached slowly.

A fine powder of $Pb_{0.85}Sn_{0.15}Te$ was made from the ingot materials by grinding in a mortar. The powder was used for XRD measurements and the remaining powder was pressed as a tablets under a pressure of 10 tones/cm^2 for SEM-EDX measurements and thin film deposition. Thin films were prepared from the ingot materials using the electron beam evaporation technique. Thick molybdenum crucible was used. The electron beam is obtained from an electron gun with an accelerating voltage of -5kV. A pre-adjustment of the deposition apparatus was made in order to obtain high quality films. The distance from the crucible to the center of the substrate holder was 19 cm and the substrates were placed in a circle of diameter 10 cm on the substrate holder and its center lies on the vertical line passing through the source of evaporation. This produces films with uniform thickness. The thicknesses of the films and the deposition rate were measured during evaporation process by using the quartz crystal thickness monitor. The films were deposited on cleaned glass substrates and singe crystals of KBr, CaF$_2$, mica, Pre-cleaned glass, polished glass by emery paper "1200". Indium metal was used as electrodes by evaporation of the indium using special masks then strengthen by silver paste. Films of x=0.15 were prepared under the following conditions:- thickness~0.8 μm, vacuum ~2×10^{-6} Torr, evaporation rate ~100 Å/sec and substrate temperatures 573 K. The films were annealed for one hour in the temperatures range 723 K. The dimensions of the Hall effect samples are 18 mm length, 2 mm width, while the dimensions of the photoconductivity samples were 10 mm width and 20 mm length. The homogeneity of the films was tested by EDX measurement at 5 points on the film surface. The relative change in the composition or Te content did not exceed 4-6 %. The structure of the samples were carried out by XRD and SEM with EDX accessory. From XRD we got the lattice parameter of the powder and films. The unit cells dimension, a(Å), is calculated from Bragg's law:-

$$a=d(h^2+k^2+l^2)^{1/2} \text{ (Å)}, \qquad (1)$$

and

$$d=\lambda/2sin\theta \qquad (2)$$

where λ=1.5405 Å is the x-ray wavelength, 2θ is the peak angle of diffraction, and d is the interplanar spacing, h,k and l are the indices. The crystallite size, D, was calculated from the width of the peak at half maximum using a reference Si single crystal. D is then given by Scherrer`s equation:

$$D = \frac{0.94\lambda}{\sqrt{\Delta_{sample}^2 - \Delta_{Si}^2} \cdot \cos(\theta)} \qquad (3)$$

Δ_{sample} and Δ_{Si}=0.051^o are the peak widths at half maximum intensity of the sample and Si, respectively. The films were studied by the Hall effect experiment. The electrical resistivity, Hall mobility and carrier concentration were measured for each films. The magnetic field of the experiment was 8 kGauss and the temperature range 100-300 K.

3. Results and discussion

3.1 Crystal structure

X-ray diffraction patterns were studied for powder, as deposited films and annealed films at 723 K as shown in Fig. 1.
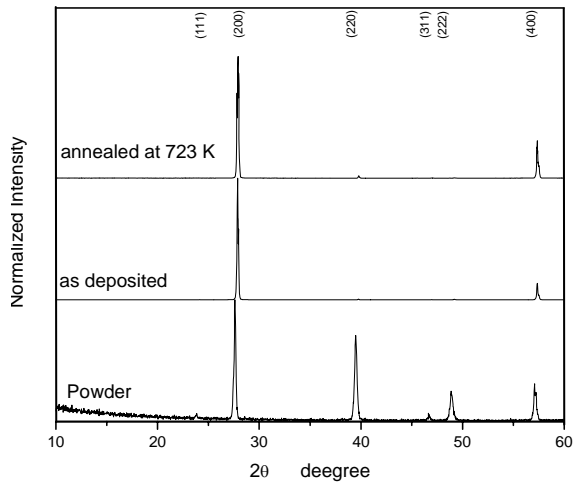
Fig. 1. XRD paterns for Pb$_{0.85}$Sn$_{0.15}$Te powder, as deposited and annealed film.

The powder and the as deposited films are polycrystalline with [200] preferred orientation of the PbSnTe crystallites for the composition with Sn$_{0.15}$. During annealing of the films the background decreases and width at half maximum decreases which indicates that the crystallite size increases. The crystallite size is increased from 50 to 60 nm.

3.2 Elemental analysis and surface morphology

The EDX measurements shows that the elemental analysis prepared powder and films. It was found that the constituent element concentration are close to the calculated weights at composition x=0.15 as shown in Table 1. The deposited films is characterized by a small deviation from the ingot composition but an excess of Te was observed due to high Te vapor pressure during the deposition process. In general the as deposited and annealed films have experimental composition of 0.18.

Table 1. EDX analysis for Pb$_{0.85}$Sn$_{0.15}$Te powder, as deposited films and films annealed at 723 K.

| Annealing temperature, K	Pb atom%	Sn atom%	Te atom%	x experimental	Te
powder	41.53	7.78	50.69	0.160	1.02
as deposited	37.67	8.27	54.06	0.180	1.18
annealed at 723 K	37.18	8.49	54.33	0.186	1.19

Scanning electron micrographs for the as deposited film and annealed films at 623 and 723 K as shown in Fig. 2. The as deposited film have no cracks or peels at higher magnification as shown in Fig. 2 (a). The effect of annealing does not improve the film quality due to appearance of cracks at annealing temperature 623 K as shown in Fig. 2 (b). Further increase in annealing temperature at 823 K determines the peeling of the film as shown in Fig. 2 (c).

(b)

(c)

(a)
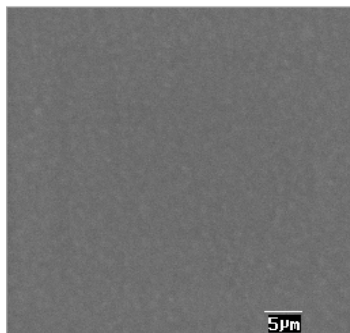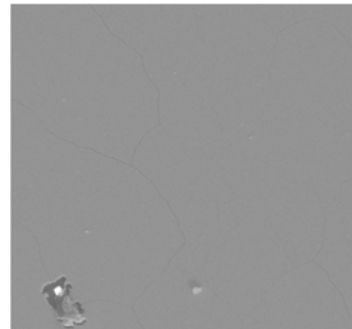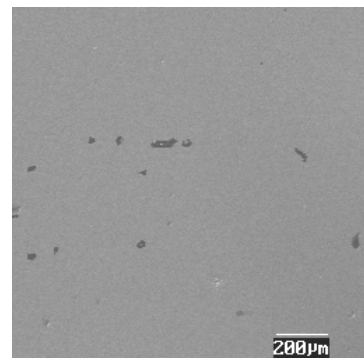
Fig. 2. (a) and (b) Film annealed at 623 K; (c) Film annealed at 823 K.

The glass substrates is not the suitable substrate for film annealing process because there is thermal stresses between the film and the glass. This comes from the large difference in thermal expansion coefficient between them ($\alpha_{glass}=8.3\times10^{-4}$ K^{-1} and $\alpha_{PbTe}=19.8\times 10^{-4}$ K^{-1}). The force between them increases at higher temperature, which make the film peel off. It can be suggested that this phenomena can be controlled by using another substrates that possess thermal expansion coefficient close to the PbSnTe material.

3.3 Electrical resistivity and conductivity

The electrical conductivity was measured in films annealed at 723 K in cooling-heating cycle in order to check the reversibility of the data. It was observed that the conductivity did not reach its initial value after one cooling-heating cycle. Each process lowers the conductivity, this means that defects are formed during heating-cooling process. Fig. 3 (a) shows the conductivity of the films cooled to 100 K and heated again to 300 K. Fig. 3 (b) shows the effect of cooling-heating process upon the conductivity at 100 and 300 K.
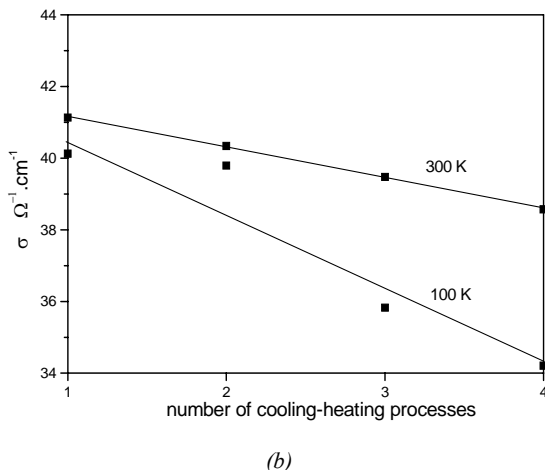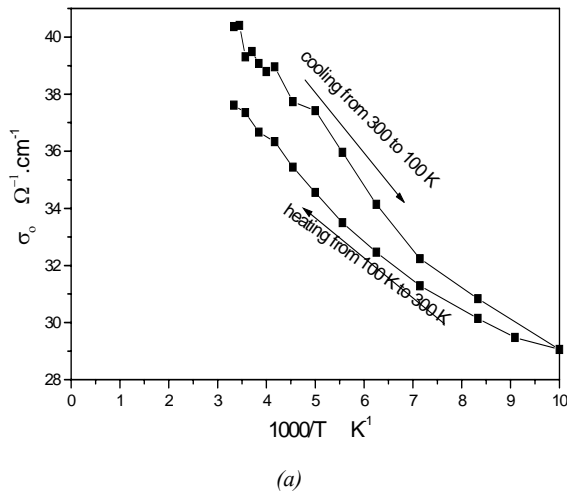

(a)

(b)

Fig. 3. Effect of cooling-heating process on the conductivity of the Pb$_{0.85}$Sn$_{0.15}$Te film annealed at 723 K.

The films were deposited on other substrates that differ in thermal expansion coefficient such as KBr, CaF$_2$, mica sheets and glass substrate. This large varieties of substrates and their surface treatment enable studying the effect of substrate type on the films quality. The films were deposited with the same preparation conditions and annealed at 723 K. Table 2 shows the thermal expansion coefficient for these substrates.

Table 2. Thermal expansion coefficient for some substrates.

Substrate	KBr	CaF$_2$	mica	glass
α_s 10^{-6} K^{-1}	38.0	19.1	14.0	8.3

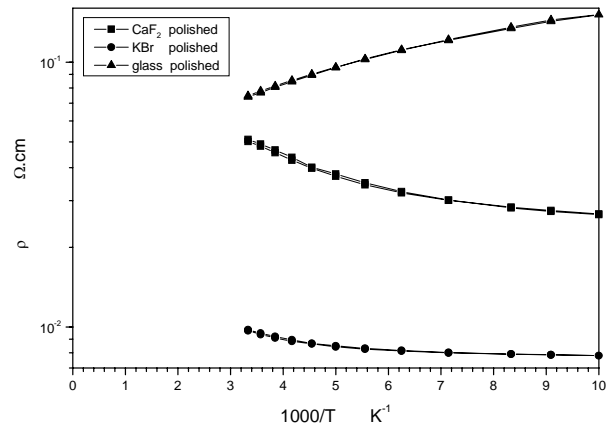The resistivity of the deposited films were measured in cooling-heating process as shown in Fig. 4.

Fig. 4. Resistivity dependence upon temperature for Pb$_{0.85}$Sn$_{0.15}$Te films deposited on different cleaved crystals, mica and glass substrates.

It is observed that the resistivity of films deposited on CaF$_2$ and KBr is $\approx10^{-2}$ Ω.cm, while films deposited on mica shows a resistivity 1.5×10^{-2} Ω.cm, and films deposited on glass have a resistivity of 0.1-0.2 Ω.cm. This means that films deposited on KBr and CaF$_2$ have the lowest resistivity. This is due to the FCC cubic structure of both KBr and CaF$_2$ which is looks like PbSnTe system. Mica exhibits a hexagonal structure which leads to lattice mismatch between the films and the substrates. Table 2 shows that the highest coefficient of the thermal expansion corresponds to KBr followed by CaF$_2$ substrates. It is shown also from Fig. 4 that the resistivity of the films increases slightly with temperature increase, indicating a semimetallic nature of the films. On the other hand, the resistivity of the films deposited on glass substrates decreases with temperature increase, indicating a semiconducting behavior. Thus the type of the substrate strongly affects the electrical resistivity of the deposited films. The effect of the polished substrates on the properties of the deposited films was also studied and Fig. 5 shows the results.
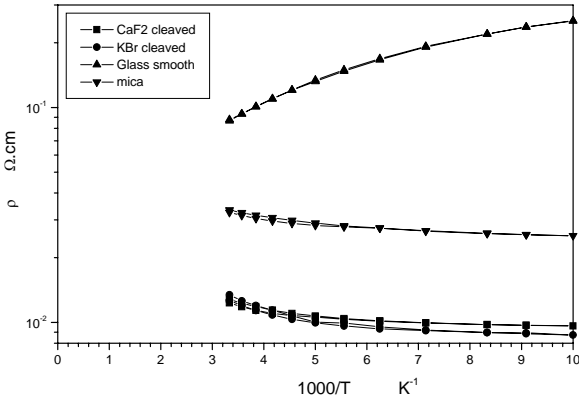
Fig. 5. Resistivity dependence upon temperature for
$Pb_{0.85}Sn_{0.15}Te$ films deposited on different polished
crystals and glass substrates.

Comparing these data with those illustrated in Fig. 4, it seems that the substrate polishing has no effect on the electrical resistivity of the deposited films. The heating cooling curves nearly coincides spatially for films deposited on KBr and CaF_2 substrates, the goal now is to deposit the films on substrates with equally thermal expansion coefficient and unit cell dimension with the same crystallographic structure in order to increase the film quality and reduce the lattice mismatch. BaF_2 satisfies these two conditions which has thermal expansion coefficient (19.8×10^{-6} K^{-1}), and unit cell dimension a=6.2 Å which is the nearest to $Pb_{0.82}Sn_{0.18}Te$ a=6.4 Å.

3.4 Galvanomagnetic properties

The carrier concentration was measured for the as deposited films and found to p-type $(1-2)\times10^{18}$ cm^{-3}. Annealing at 723 K for one hour produces films with mixed carriers, the carriers type changed from p-type to n-type at temperature range 200-220 K with the carriers concentration of 3×10^{18} cm^{-3}.

The Hall mobility was measured for films deposited on the mentioned different substrates as shown in Fig. 6. It is observed that the carriers mobility of films deposited on KBr (cleaved and polished) and CaF_2 substrates are in the range $(3-4)\times10^3$ $cm^2V^{-1}s^{-1}$. Polishing CaF_2 substrates produces films of lower mobility than the freshly cleaved substrates ($\approx10^3$ $cm^2V^{-1}s^{-1}$). The lowest carriers mobilities corresponds to glass substrates, which is in the ranges $(0.5-3)\times10^2$ $cm^2V^{-1}s^{-1}$. The carrier mobility increases as temperature increases until temperature range 180-200 K, then decreases with increasing the temperature.
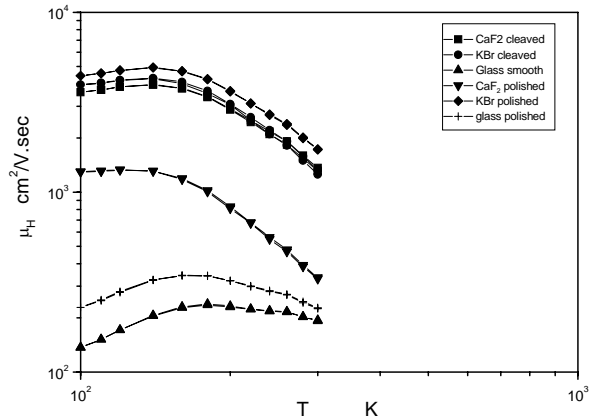

Fig. 6. Hall mobility dependence upon temperature for
$Pb_{0.85}Sn_{0.15}Te$ films deposited on different substrates.

Concerning films deposited on glass (smooth and polished) substrates, the carriers mobility increases with increasing temperature from 100 to 400 K. This explains the decrease of the resistivity of those films with increasing the temperature. A slight decrease of the carriers mobility at higher temperature may be followed by carriers increase with heating, which leads to the decrease of the resistivity. Table 3 shows the slope of μ-T curves in log scale for films deposited on different types of substrates. The slope of the curves for films deposited on mica, CaF_2 and KBr monocrystalline substrate ranges from 2.0 to 1.5.

Table 3. The slope of μ-T curves.

Substrate	CaF_2 cleaved	CaF_2 polished	KBr cleaved	KBr polished	Mica	Glass normal	Glass polished
Slope	-1.616	-2.089	-1.816	-1.52	-1.564	-0.394	-0.67

The negative slopes indicate a scattering process, which increases with heating. This scattering may be due to acoustic phonon scattering. The negative slope for carriers mobility of films deposited on glass substrates represents the behavior in the temperature range 200 K and higher may be due to the higher carriers concentration in the conduction band at this temperature range, leading to collisions, which decreases the mobility. The decrease of the mobility with heating was explained by phonon scattering.

3.5 Photoconductivity

The photoconductivity-temperature relationship of $Pb_{0.85}Sn_{0.15}Te$ films deposited on different substrates is shown in Fig. 7.
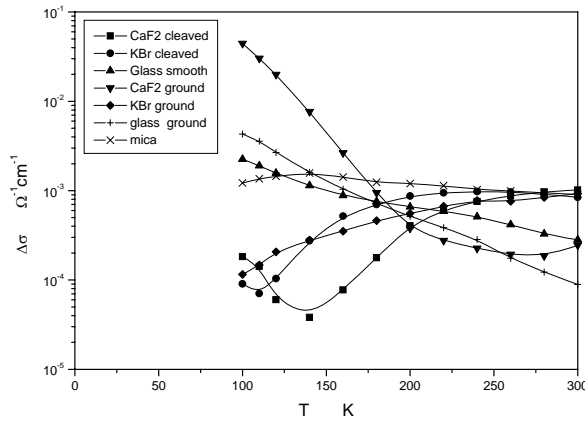
*Fig. 7. Photoconductivity dependence upon temperature
for films deposited on different substrates.*

The photoconductivity is nearly unchanged with temperature for films deposited on mica sheet. The photoconductivity for films deposited on polished and cleaved CaF_2 crystals have nearly the same behavior with temperature, it decreases as the temperature decreases. The photoconductivity of films deposited on polished CaF_2 crystals increases by 3-4 orders of magnitude at 100 K. The variation of the photoconductivity with temperature of films deposited on cleaved substrates increases from 10^{-4} $\Omega^{-1}cm^{-1}$ to 2×10^{-2} $\Omega^{-1}cm^{-1}$ as the temperature decreases from room temperature to 100 K. On the other hand the photoconductivity decreases from 10^{-3} $\Omega^{-1}cm^{-1}$ to 10^{-4} $\Omega^{-1}cm^{-1}$ for films deposited on polished CaF_2 substrates as the temperature decreases from room temperature to   100 K.

The photoconductivity of films deposited on KBr substrates decreases from 10^{-3} $\Omega^{-1}cm^{-1}$ to 10^{-4} $\Omega^{-1}cm^{-1}$ as the temperature decreases from 300 K to 100 K. Hence the polishing of the KBr substrate has no effect on the photoconductivity, while it is effective in CaF_2. The photoconductivity of films deposited on smooth and polished glass has the same behavior where they increase as the temperature decreases. The photoconductivity increases from $\approx 10^{-3}$ $\Omega^{-1}cm^{-1}$ to 3×10^{-3} $\Omega^{-1}cm^{-1}$ as the temperature decreases from 300 to 100 K. But the increase of photoconductivity with cooling for films deposited on glass substrates is less than that for films deposited on CaF_2 substrates which is strange result because the quality of films deposited on CaF_2 is better than those on glass. This leads us to examine whether the obtained photosignal comes from the photocarriers or includes heat effect.

Suppose that the photo-signal consists of two components:

1-Pure photoconductivity component, which depends only on the change in conductivity due to photo-carriers (internal photo-effect). The a.c. photoconductivity relationship is given by [15]:

$$\Delta\sigma_{ac} = \frac{wd}{l} \Delta\sigma_{st} \frac{1-e^{-t_o/\tau}}{1+e^{-t_o/\tau}} = \frac{wd}{l} \Delta\sigma_{st} \tanh\frac{t_o}{2\tau} = \frac{A}{l} \Delta\sigma_{st} \tanh\frac{1}{4\tau f} \quad (4)$$

where $\Delta\sigma_{ac}$ is the photoconductivity, w is the width, d is the thickness, l is the length of the film, τ is the carriers lifetime and f is the frequency of the light. 2-Apparent photoconductivity which is due to a heat pulses, which come from the illumination of the sample under poor heat sink. As a result, the film conductivity change momentally, since the film thermal capacity is very small.

Assuming that the conductivity at temperature T_1 is σ_1 and that at temperature T_2 is σ_2 due to heating by illumination), then the apparent photoconductivity, $\Delta\sigma_{heat}$ is then given by:

$$\Delta\sigma_{heat} = \sigma_2 - \sigma_1 \quad (5)$$

The temperature of the film is changed momentally by $\Delta T = T_2 - T_1$ due to illumination. Therefore it can be considered that we are dealing with the variation of the dark conductivity with temperature in a short time due to low heat capacity of the film. The slope of such curve is equal to $\Delta\sigma/\Delta T$ and its infinitesimal change is equal to $d\sigma/dT$. Therefore

$$\Delta\sigma_{heat} = (d\sigma/dT).\Delta T \quad (6)$$

where $d\sigma/dT$ is the slope of the σ-T curve.

The equilibrium heat equation due to illumination of the film and the heat sink from the substrate is given by: under illumination

$$\frac{dQ}{dt} = AJ - \beta(T - T_o) \quad (7)$$

in darkness

$$\frac{dQ}{dt} = -\beta(T - T_o) \quad (8)$$

where dQ/dT is the change of the quantity of heat with time, A is the light incidence area, J is the incident light power, β is the thermal conductivity between the film and the substrate (from the film to heat sink), T is the temperature of the film and T_o is the temperature of the substrate.

In the best conditions, if the matching between the film and the substrate is good, this leads to a good heat sink from the film to the substrate. In this case the film and the substrate temperatures will be the same. In the worst case, when the film and the substrate are mismatched, this leads to poor heat sink from the film to the substrate and consequently a temperature difference between the film and the substrate is found.

Suppose that there is a mismatch between the film and the substrate. Let $Q=mC\Delta T$, is the quantity of head absorbed by the films which increase its temperature by $\Delta T = T_1 - T_2$, m is the film mass, C is its specific heat of the film, Eqns.(7, 8) will be modified to:

under illumination

$$mC\frac{d\Delta T}{dt} = AJ - A\beta.\Delta T \quad (9)$$

in darkness

$$mC\frac{d\Delta T}{dt} = -A\beta\Delta T \qquad (10)$$

Dividing by mC in both equations and put by $\tau_{heat} = A\beta/mc$. We get:

$$\frac{d\Delta T}{dt} = \frac{AJ}{mc} - \frac{\Delta T}{\tau_{heat}}$$

$$\frac{d\Delta T}{dt} = -\frac{\Delta T}{\tau_{heat}}$$

Separating the variables and integrating, we get the general solutions of the above differential equation. Using the boundary conditions t=∞ and t=0 in order to determine the constants.

Under illumination

$$\Delta T = \frac{AJ\tau_{heat}}{mc}(1-e^{-t/\tau_{heat}}) = \frac{J}{\beta}(1-e^{-t/\tau_{heat}}) \qquad (11)$$

Under darkness

$$\Delta T = \frac{J}{\beta}e^{-t/\tau_{heat}} \qquad (12)$$

Eqns.(11) and (12) are true only when the chopping frequency is too small to return the film to its initial temperature T_o again. In real case ΔT does not reach its steady-state value and in darkness the temperature does not start from T_o. The treatment of these equations is similar to that was made for frequency dependence of photoconductivity in Chapter (3) reference [15], in this reference also the Eqn.(4) are deduced. The alternative change in temperature due to illumination is then given by the frequency of the chopped light instead of the time duration of the incident light pulse, the alternative change in film's temperature is given by:

$$\Delta T = \frac{J}{\beta}\tanh\frac{1}{4f\tau_{heat}} \qquad (13)$$

an a.c. signal in this case is produced when an external voltage is applied due to change in the film conductivity. The conductivity depends upon temperature as: σ =σ(T). Then the change in conductivity due to heat is given by substitution in Eqn(6):

$$\Delta\sigma_{heat} = \frac{d\sigma}{dT}.\Delta T = \frac{d\sigma}{dT}.\frac{J}{\beta}\tanh\frac{1}{4f\tau_{heat}} = const\tanh\frac{1}{4f\tau_{heat}} \qquad (14)$$

Eqn.(14) shows some properties of this type of the heat effect:

1-Its behavior looks like the normal photoconductivity (obtained from the photo carriers). The source of photo signal is not due to photo carriers in this case but from the change of applied voltage across the film by heating.

2- $-\Delta\sigma_{heat}$ vanishes when β is high (high thermal conductivity between the film and the substrate), or at high heat capacity of the film (either specific heat or the film mass) so that we don't get $\Delta\sigma_{heat}$ for bulk samples because of good heat sink and high mass.

3-$\Delta\sigma_{heat}$ is not a low process, because the mass of the film is too small to be heated quickly from the incident light pulse and is cooled slowly from the substrate due to a poor heat sink.

4-$\Delta\sigma_{heat}$ depends upon the specific heat of the film and the thermal conductivity between the film and the substrate. This interface is mainly depends on the growth and heat treatment. If the thermal expansion coefficient of the film differs from the substrate, they separates with heating due to thermal stresses and produces spaces and peals, which decreases the heat rate flow.

5- $\Delta\sigma_{heat}$ has no advantages, because it is not a material characteristic only but also growth and substrate properties and every heating-cooling cycle increase this types of defects which affect on the life time of the device. Most of IR photoconductors or detectors works at low temperature, this means that the life time of the detector is small besides its characteristics changes with each cooling process. In earlier work we studied the effect of the substrate temperature on the film preparation [16]. Some difficulties were found in film properties when the films were deposited at higher substrate temperatures

By applying the mentioned model in our case in order to know whether the measured photoconductivity in all films is due to photo-carriers or heat effect. The heat effect photoconductivity component is directly proportional to the first derivative of the dark conductivity. The photoconductivity and the first derivative of the dark conductivity dependence upon the temperature are represented in Fig. 8 and Fig. 9.
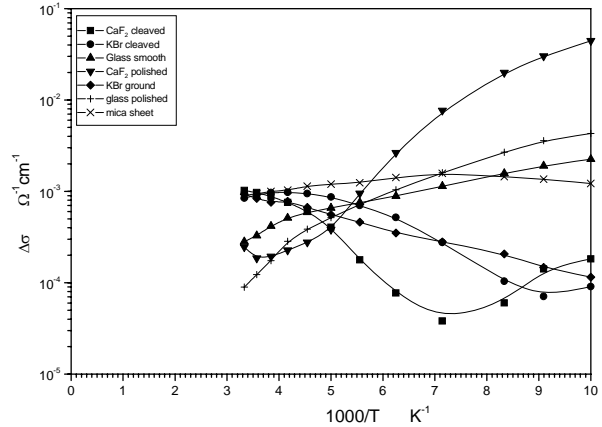

Fig. 8. Photoconductivity dependence upon temperature for films deposited on different substrates.
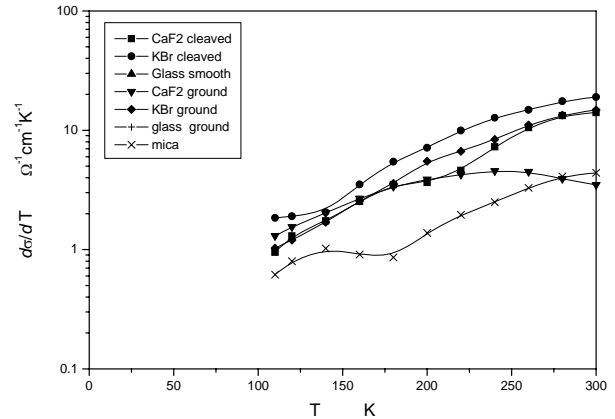

Fig. 9. The first derivative of dark conductivity for films deposited on different substrates.

It is shown that there is no relation between them especially, in the sensitive region of the low temperature 100-180 K. The behavior of the temperature dependences of the measured photoconductivity and the first derivative of the dark conductivity are far from each other. This means that the photoconductivity component due to the heat effect is very small and the change of the photoconductivity with temperature is due to the photo-carriers. This discussion leads to an important result. A part of the photoconductivity may occur due to heat. But only occurs in the high temperature range where the measured photoconductivity is very small if compared with the photoconductivity at low temperature. Therefore the change of the photoconductivity with temperature is mainly due to $\mu\tau$ product.

From the previous and present work, the following consideration should be taken into account when the preparation conditions are optimized.

1-The substrate should possess equally or nearly equally thermal expansion coefficients such as PbTe-SnTe alloy in both high and low temperature ranges

2-Their lattice constants match well with film lattice constant in order to decrease the stresses on the film by epitaxial growth.

3-The substrate have high thermal conductivity.

4-The dimensions of the films can be designed to be small in order to minimize the cracks due to the difference between the thermal expansion coefficients of the film and the substrate.

The above considerations show that glass substrates are not suitable because they have low thermal expansion coefficient. Moreover, glass is amorphous and consequently the deposited film will be poor crystalline.

Mica substrates has hexagonal structure and its thermal expansion coefficient is quite smaller than PbTe. KBr substrates have thermal expansion coefficients twice times of magnitude of PbTe but KBr has cubic structure, which is similar to that of PbTe and PbSnTe alloy. The other substrates have thermal expansion coefficient near to PbSnTe thermal expansion coefficient at room temperature such as CaF_2 ($19.1 \times 10^{-6} K^{-1}$, $a = 5.464$) and BaF_2 (19.8×10^{-6} K^{-1}, $a = 6.200$) but there is a little information about the thermal expansion coefficient at low temperatures. They may give better results when they are used as substrates or buffer layers between the substrates and the films.

The use of BaF_2 substrates has three advantages:

1-Considerable high thermal conductivity such that the change of the film temperature during measurements is negligible.

2-The thermal expansion coefficient of such crystals is nearly the same as that of PbSnTe films.

3-The lattice constant of BaF_2 is near to those in PbSnTe films, and they have the same crystallographic structure. This reduces the stresses between the film and the substrate which helps in obtaining epitaxial films. These films have the highest conductivity due to their highest Hall mobility. Besides BaF_2 is IR transparent until 25 μm so that the films can be illuminated from the back side of the substrate.

The above preparation conditions were optimized for composition x=0.15. These preparation conditions were applied on high composition x=0.4 and low composition x=0.00. Every composition needs different substrate temperature and annealing temperature. The preparation conditions are controlled by the effect of substrate temperature, annealing temperature and the annealing time. The parameter that measures the best preparation conditions is the minimum carrier concentration. By using BaF_2 substrates, Fig. 10 and Fig. 11 show the dependence of the photoconductivity upon wavelength for $Pb_{1-x}Sn_xTe$ films where x=0.00 and 0.35, respectively.
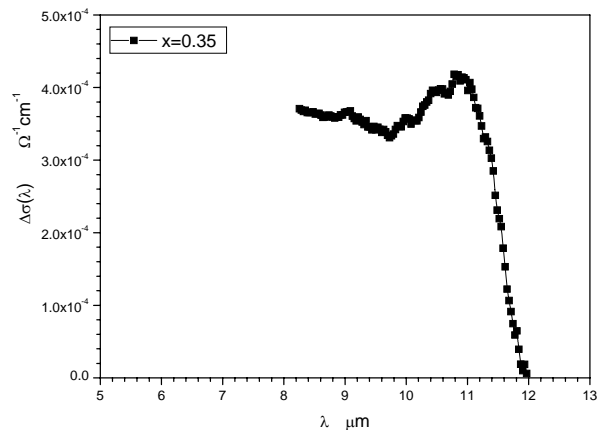
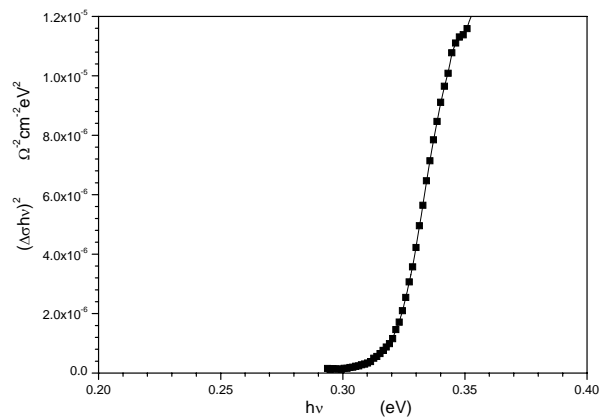*Fig. 10. Photoconductivity dependence upon wavelength for film of composition x=0.00 deposited on BaF_2 substrate.*

Fig. 11. Photoconductivity dependence upon wavelength for film of composition x=0.35 deposited on BaF_2 substrate.

It appears that the absorption edge is sharp. Fig. 12 shows the $(\Delta\sigma h\nu)^2$ dependence upon $h\nu$ for film as a representative curve used for calculation of the band gap (the same treatment of the absorption coefficient because the photoconductivity is directly proportional to the absorption coefficient in the fundamental absorption region, the PbSnTe is direct band gap).
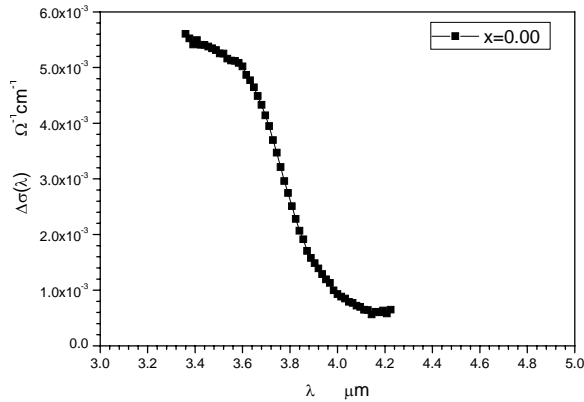
Fig. 12. $(\Delta\sigma h\nu)^2$ dependence upon $h\nu$ for PbTe film x=0.0.

It is observed that the experimental and theoretical calculated E_g are close to each other.

4. Conclusions

PbSnTe films are photo-sensitive in the IR region of the spectrum. Optimization of the growth conditions, heat treatment and substrate type must be taken into account. BaF_2 single crystal substrate is more suitable for obtaining IR photoconductors detectors when it is used as substrates. Annealing in good substrates such as BaF_2 increase the quality of the photoconductor and its sensitivity. Also BaF_2 is not soluble in water and is not affected by humidity, which makes the IR PbSnTe photoconductor to work for a longer period. The PbSnTe photoconductors work in different spectral regions depending on the composition and working temperature. The band gap can be tuned by composition and finely tuned by temperature.

The theoretically calculated band gap and the experimentally obtained from the $(\Delta\sigma h\nu)^2$- $h\nu$ relationship at different compositions and temperatures are represented in Fig. 13 and Fig. 14.
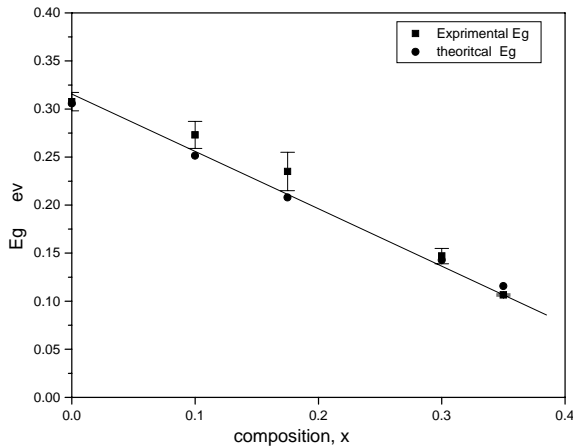

Fig. 13. Theoretical and experimental band gap for $Pb_{1-x}Sn_xTe$ films deposited on BaF_2 crystals dependence upon composition.
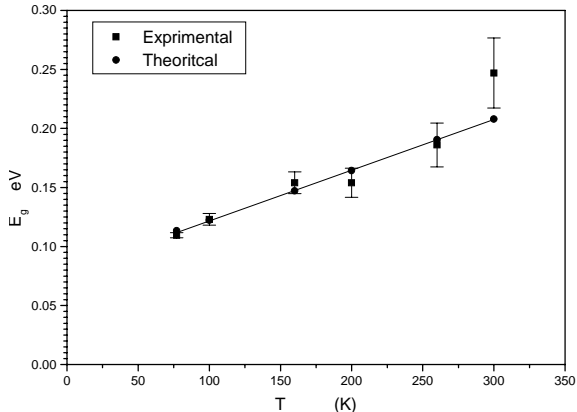

Fig. 14. Theoretically and experimentally calculated band gap at different temperatures for films with x=0.15 deposited on BaF_2 substrate.

References

[1] S. P. Yordanov, Part I, Bulgarian J. of Physics. **17**, 507 (1990) .
[2] S. P. Yordanov, Part II, Bulgarian J. of Physics **18**, 15 (1991).
[3] E. P. Skipetrov, A. N. Nekrasova, L. A. Skipetrova, L. I. Ryabova, Proceeding of SPIE-The International Society for Optical engineering **3182**, 228 (1996) .
[4] P. Dariel, Z. Dashevsky, A. Jarashnely, S. Shusterman, A. Horowitz, J. Crystal Grouth **234**, 164 (2002).
[5] S. P. Zimim, M. N. Preobrazhensky, D. S. Zimin, R. F. Zaykina, G. A. Borzova, V. V. Naumov, Infrared Phys. and Technol. **40,** 337 (1999).
[6] J. H. Myers, R. H. Morriss, R. J. Deck, J. Appl. Phys. **42**, 5578 (1971).
[7] K. Weiser, A. Klein, Ainhorn, J. Appl. Phys. Lett. **34**, 607 (1979).
[8] P. J. A. Zoutendyk, Proceeding of the Conference Held at Dallas, Texas in (20-21March) **32**, 421 (1970).
[9] V. B. Oiletski, F. F. Sizov, G. V. Lashkarev, K. D. Tovstyuk, Physics and Technics of Semiconductors, **8,** 269 (1975).
[10] K. W. Nill, J. N. Walpole, A. R. Calawa, T. C. Harman, Proceeding of the Conference Held at Dallas, Texas in (20-21March) **32,** 383 (1970).
[11] H. Zogg, C. Maissen, J. Mashino, S. Blunier, A. N. Tiwarl, J. Semicond. Sci. and Technol. **6,** C6 (1991).
[12] D. R. Khokhlov S. N. Raines, D. M. Watson, I. I. Ivanchik, J. Pipher, J. Appl. Phys. Letters **76**, 2835 (2000).
[13] K. Alchalabi, H. Zogg, D. Zimin, K. Kellermann, Proc. 11th Tnternationl Workshop on Physics of Semiconductorsdevices, Delhi, Dec. 11-15 IWPSD, 21 (2001).
[14] K. Alchalabi, D. Zimin, H. Zogg, W. Buttler, IEEE Electron Device Letters. **22,** 110 (2001).

[15] S. M. Ryvkin, Photoelectric Effect in
Semiconductors, authorized translated from Russion
to English by A. Tybulewich, B. Sc A. Inst. P, M. I.
Inf. Sc, Fil.(c/b) consultants Bureau, New yourk,
1964.

[16] M. Abdel Rafea, F. S. Terraa, M. Mounir, R.
Labusch, Chalcogenide Letters **6**, 115 (2009).

_____
*Corresponding author: m.abdelrafea@mucsat.sci.eg